ISSN 2411-3336; e-ISSN 2541-9404

JOURNAL OF MINING INSTITUTE

Zapiski Gornogo instituta

Journal homepage: pmi.spmi.ru

Research article

Quantitative determination of sulfur forms in bottom sediments for rapid assessment of the industrial facilities impact on aquatic ecosystems

Ivan P. Sverchkov✉, Vladimir G. Povarov

Empress Catherine II Saint Petersburg Mining University, Saint Petersburg, Russia

***How to cite this article*:** Sverchkov I.P., Povarov V.G. Quantitative determination of sulfur forms in bottom sediments for rapid assessment of the industrial facilities impact on aquatic ecosystems. Journal of Mining Institute. 2024. Vol. 267, p. 372-380.

Abstract. The article describes an X-ray fluorescence method for quantitative analysis of sulfate and total sulfur in bottom sediments of watercourses and reservoirs located in the area of industrial enterprises impact. The quantitative determination of sulfur forms was carried out by analyzing the characteristic curves $SK\alpha_{1,2}$ and $SK\beta_{1,3}$, as well as the satellite line $SK\beta'$ on X-ray emission spectra measured by an X-ray fluorescence spectrometer with wavelength dispersion. The study shows that these characteristic curves allow not only to determine the predominant form of sulfur, but also to separately conduct quantitative analyses of sulfates and total sulfur after fitting peaks and to separately analyze overlapping spectral lines. The results of quantitative analysis of the chemical state of sulfur by the proposed X-ray fluorescence method were compared with the results of inductively coupled plasma atomic emission spectroscopy and elemental analysis, as well as certified standard samples of soils and sediments. The results are in good agreement with each other.

***Keywords*:** bottom sediments; sulfur; sulfates; X-ray fluorescence analysis; fitting peaks; satellite lines; quantitative analysis

Acknowledgment. The work was carried out under the state assignment of the Ministry of Science and Higher Education of the Russian Federation (FSRW-2024-0005).

Received: 16.04.2024 ***Accepted: 03.06.2024*** ***Online: 04.07.2024*** ***Published: 04.07.2024***

Introduction. Sulfur is one of the most important elements of various components of the natural environment. It is also a necessary element for soils and plants, since it is a component of amino acids and enzymes that are vital for the livelihood of organisms and for metabolism in soils. However, an excess of sulfur in the soil can contribute to its acidification, inflict damage on plants and slow down their growth [1-3]. Also, sulfur can serve as one of the indicators of environmental pollution resulting from discharges and emissions of industrial enterprises. Analysis of the content and forms of sulfur in sediments and soils allows us not only to assess the ecological state, but also to develop measures to reduce pollution [4-6]. At the sediment-water interface, sulfur in bottom sediments undergoes a complex geochemical process before it finally forms a stable compound. The study of the content and forms of sulfur in the bottom sediments of water bodies is of great ecological importance for the early diagnosis of their contamination with heavy metals and control of the chemical composition of water [7-9].

Data on the chemical state of sulfur is also necessary for geochemical studies in the analysis of ores. Information about the content of sulfides and sulfates is important in assessing the genesis of the deposit and determining its industrial value. The method that is usually used to determine the forms of sulfur is the laborious gravimetric method with the sequential dissolution of sulfur-containing compounds and further precipitation of sulfates in the form of $BaSO_4$ [10-12].

XRF is one of the most universal analytical methods for studying the elemental composition of objects of different composition. The method does not require time-consuming and expensive stages of

sample preparation [13-15]. As noted in the studies [16-18], the position and shape of the SKα и SKβ lines for sulfur can vary greatly depending on the degree of oxidation of this element. The presence of various types of satellite lines on the spectra is explained by various processes and effects: multiple ionization, exchange interaction, plasmon excitation, radioactive Auger effect and molecular orbitals [19]. Also, the structure of the characteristic X-ray spectrum is affected by the valence and the compound the atom is in. For sulfur, this effect is more significant in the area of the SKβ line than in the area of the SKα, since the SKβ lines arise as a result of transitions that involve 3p-orbital, which is more external than the 2p-orbital associated with the SKα line. The intensities and widths of the forbidden and satellite SKβ lines depend on the concentration and degree of oxidation of sulfur atoms. These spectra differences can be used for qualitative and quantitative analysis of sulfur forms, which can significantly reduce the analysis time [20].

Methods. *Chemical reagents*. To study the spectra of pure sulfur compounds having different degrees of oxidation, we used high purity elemental sulfur (AO REAChem, Moscow, Russia), chemically pure anhydrous sodium sulfate (AO LenReactiv, Saint Petersburg, Russia) and 99.9 % iron disulfide (Sigma-Aldrich Co. LLC, Saint Louis, USA).

When studying the effect of the cation on the intensity of peaks $SK\beta_{1,3}$ и SKβ′ samples of sulfates of various metals with a mass sulfur content of 2 % were prepared from chemically pure reagents: $CaSO_4$, $CuSO_4$, $FeSO_4 \cdot 7H_2O$, $KAl(SO_4)_2 \cdot 12H_2O$, $MgSO_4$, Na_2SO_4 (AO LenReactiv).

Sample preparation. To calibrate the wavelength dispersive X-ray fluorescence spectrometer, a set of 9 samples of artificial mixtures obtained by mixing sulfur-free rock and pure anhydrous calcium sulfate was prepared. The composition of the sulfur-free rock, on the basis of which artificial reference samples were made, wt.%: SiO_2 – 58.9; Al_2O_3 – 16.8; K_2O – 5.59; Fe_2O_3 – 5.05; Na_2O – 4.49; CaO – 3.58; MgO – 3.23; TiO_2 – 0.95; P_2O_5 – 0.25; MnO – 0.06; LOI < 0.01.

The samples of soil and calcium sulfate previously dried in a drying cabinet (ED 23, Binder, Tuttlingen, Germany) were weighed on electronic scales (MSE124S-1CE-DU, Sartorius, Göttingen, Germany) and thoroughly homogenized using a mixing device (Ultra Turrax, IKA, Staufen, Germany). The samples were prepared by pressing the samples with a binder into reusable steel rings with a diameter of 32 mm using an automatic press (PP 40, Retsch, Haan, Germany) with a maximum pressing force of 25 tons.

To check the calibration dependencies, 8 samples were taken, a standard sample of bottom sediments with a certified total sulfur value (SGHM-4, Vinogradov Institute of Geochemistry SB RAS, Irkutsk, Russia), a standard rock sample with an approximate sulfur content (SP89, Rocklabs, Dunedin, New Zealand), 4 samples of bottom sediments and 2 samples of copper ore enrichment waste. Sample preparation was carried out in the same way as for artificial mixtures.

Determination of sulfur spectra. A scanning wavelength dispersive X-ray fluorescence spectrometer (XRF-1800, Shimadzu, Kyoto, Japan) with a power up to 4 kW equipped with an X-ray tube with Rh anode was used to obtain the spectra of the prepared samples. The parameters of the spectrometer operation for the studies carried out in the work: X-ray fluorescence spectrometer – XRF-1800 (Shimadzu); material of the X-ray tube anode – rhodium (Rh); Voltage/current of the X-ray tube – 25 kV/100 mA; crystal analyzer – Ge (2d-6.532 Å); scanning range – 98.5-112.5 degree (2.283-2.505 keV); scan step – 0.05 degree; total scan time – 840 s; detector – FPC; collimator diameter – 30 mm; atmosphere – vacuum.

Determination of total sulfur and sulfates. The total sulfur concentrations in all samples were determined using an elemental analyzer (628S, LECO, Michigan, USA) by analyzing the composition of gases formed after complete combustion of the sample at a temperature of 1450 °C. The measurements were carried out in accordance with ISO 15178:2000. Soil quality – Determination of total sulfur by dry combustion. To determine the content of sulfates, the samples were boiled in a 15 % hydrochloric acid solution. Then the solution was filtered, the filter and the precipitate were repeatedly washed with hydrochloric acid. The resulting solution was analyzed by inductively coupled plasma atomic emission spectroscopy (ICPE-9000, Shimadzu).

Results and discussion. *Investigation of spectral lines of various types of sulfur.* Sulfur has different degrees of oxidation, S^{-2}, S^{-1}, S^{0}, S^{+1}, S^{+2}, S^{+4} и S^{+6}. However, native (S^{0}), sulfide (S^{-2}) and sulfate (S^{+6}) forms are most often found in nature [21, 22]. With the help of WDXRF, spectral lines of sulfur with different valence can be observed. As can be seen in Fig.1, the lines $SK\alpha_{1,2}$ и $SK\beta_{1,3}$ are observed for all types of sulfur, and the satellite line SKβ′ is characteristic of sulfates. Along with the additional spectral line SKβ′, a shift of the main peak $SK\alpha_{1,2}$ by about 2 eV, towards lower energies is also observed for sulfates [23]. Such a slight shift of the analytical line is difficult to interpret for determination of the type of sulfur.

Determination of total sulfur by analyzing the intensity of the $SK\alpha_{1,2}$ line is a routine operation [14, 15, 24], therefore, further attention will be paid to the quantitative determination of sulfates in samples containing various types of sulfur and will focus on the analysis of the characteristic lines $SK\beta_{1,3}$ and SKβ′. As can be seen from Fig.1, the peak of the SKβ sulfate ion has two main components, $SK\beta_{1,3}$ и SKβ′, in contrast to elemental and sulfide sulfur. This is due to the fact that the SKβ region of the sulfur line significantly depends on the degree of oxidation. For pure sulfur, the main transition of $SK\beta_{1,3}$ corresponds to a peak formed by two lines caused by molecular orbitals that bind different levels of the S_8 molecule [25], and in oxides it is associated with the transition of electrons from the molecular orbital consisting of the atomic orbitals 3p of sulfur and 2p of oxygen to the 1s orbital of sulfur. Thus, the difference between the transitions $SK\beta_{1,3}$ и SKβ′ is determined by the atomic orbital of the ligand involved. Therefore, the energy difference is approximately determined by the energy difference of the 2s and 2p orbitals of the ligand, which for oxygen is approximately 15 eV [18, 19, 26].

Along with the $SK\beta_{1,3}$ and SKβ′, lines, the spectra in the region selected for analysis may contain the $SK\beta_x$ and SKβ″ lines. However, SKβ″ is not characteristic of sulfates, and $SK\beta_x$ is not observed on the spectra obtained using WDXRF due to insufficient resolution [27, 28]. For these reasons, the analysis of these characteristic lines was not carried out.

Fitting peaks. Overlapping peaks of $SK\beta_{1,3}$ and SKβ′ are difficult to analyze without preprocessing (Fig.1). This is especially difficult for cases when the sample includes a mixture of various compounds containing sulfur, in which case the main peak of $SK\beta_{1,3}$ can raise several times higher relative to SKβ′ and cover the satellite line even more. For this reason, peak fitting was further used for all spectral lines (OriginPro, OriginLab Corporation, Northampton, USA). An example of a decoded peak after the fitting is shown in Fig.2. The position of the spectral lines $SK\beta_{1,3}$ and SKβ′ at 2,464 and 2,452 keV respectively, agrees well with the values obtained in other studies where devices with better resolution were used [18, 29, 30].

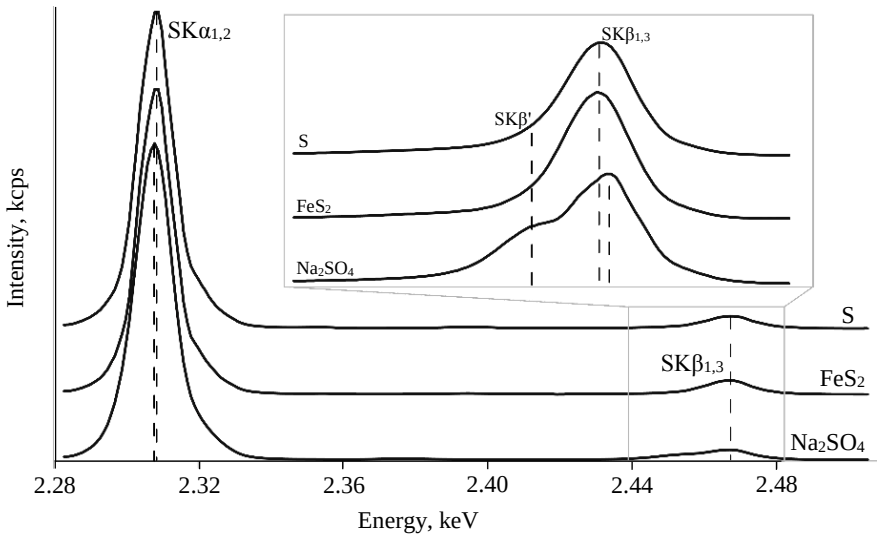

Fig.1. X-ray spectra of various sulfur compounds

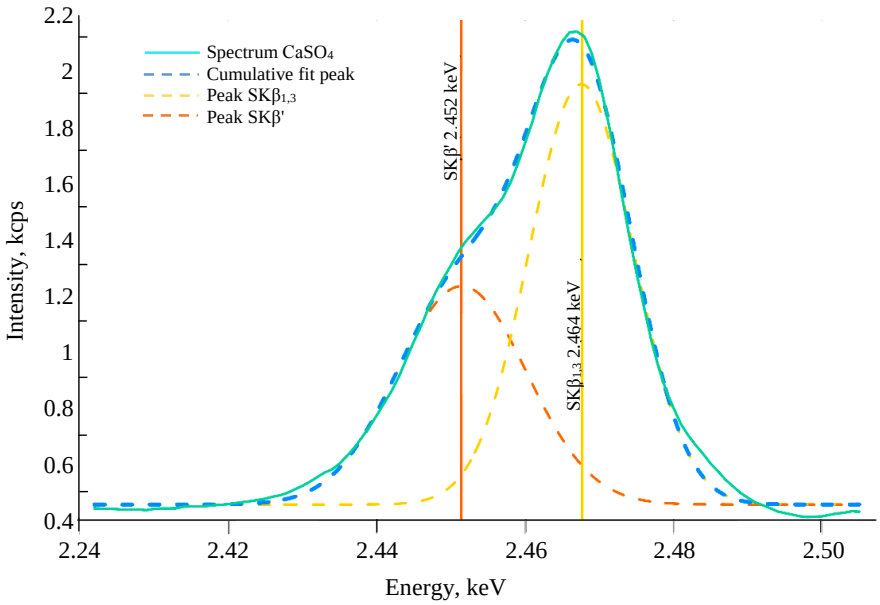

Fig.2. X-ray spectrum after fitting for a sample with a sulfur sulfate content of 1 wt.%

Gaussian function was used to fit the peaks. The function has the following equation

$$y = y_0 + \frac{A \cdot e^{\frac{-4\ln(2)(x-x_c)^2}{w^2}}}{w\sqrt{\frac{\pi}{4\ln(2)}}},$$

where y_0 – the height of the baseline; x_c is the position of the peak center; A – the area under the peak; w is the width of the peak at half of its height [31, 32].

Using the Gaussian function to fit the peaks provided a correlation between the initial and the total spectrum. The total spectrum was obtained after adding the peaks SKβ$_{1,3}$ and SKβ′, more than 0.995 for each of the experiments.

Effect of the cation in sulfates on the intensity ratio of SKβ′/SKβ$_{1,3}$. The ratio of the intensity of the lines and the areas under the peaks SKβ′ and SKβ$_{1,3}$ carries information about the form in which sulfur is contained in the sample only in the form of sulfates or other compounds. As shown in the conducted studies [26, 33], the ratio of the intensities of the SKβ′ satellite line to the main SKβ$_{1,3}$ line in the sample correlates with the concentration of sulfates in the sample.

To confirm that the cation does not significantly affect the intensity ratios of the lines (areas under the peaks) SKβ′ и SKβ$_{1,3}$, samples were prepared (sulfates of various metals with a mass sulfur content of 2 %), and the intensity ratios (excluding background) and peak areas (excluding background) of the selected analytical lines were determined, SKβ′/SKβ$_{1,3}$ (Table 1). The ratios of intensities and peak areas of SKβ′/SKβ$_{1,3}$ for sulfates having different cations remain the same. The largest deviation from the average value for the intensity ratio was 2.83 % and for the areas ratio it was 1.75 %, which means that the influence of the cation on the sulfur spectrum is insignificant. This is due to the fact that in the ions of polyatomic compounds, individual ionic groups, for example SO_4^{2-}, are isolated anions and they are not significantly affected by cations [30, 34]. Thus, the influence of the cation on the intensity of the characteristic sulfur lines in the SKβ region will be insignificant and will have no recognizable effect on the quantitative determination of sulfates in real samples.

Table 1

Intensity ratio of SKβ′/SKβ$_{1,3}$

Salt	Intensity	Area
$CaSO_4$	0.526	0.627
$CuSO_4$	0.515	0.632
$FeSO_4 \cdot 7H_2O$	0.500	0.616
$KAl(SO_4)_2 \cdot 12H_2O$	0.507	0.623
$MgSO_4$	0.511	0.636
Na_2SO_4	0.510	0.628

Journal of Mining Institute. 2024. Vol. 267. P. 372-380

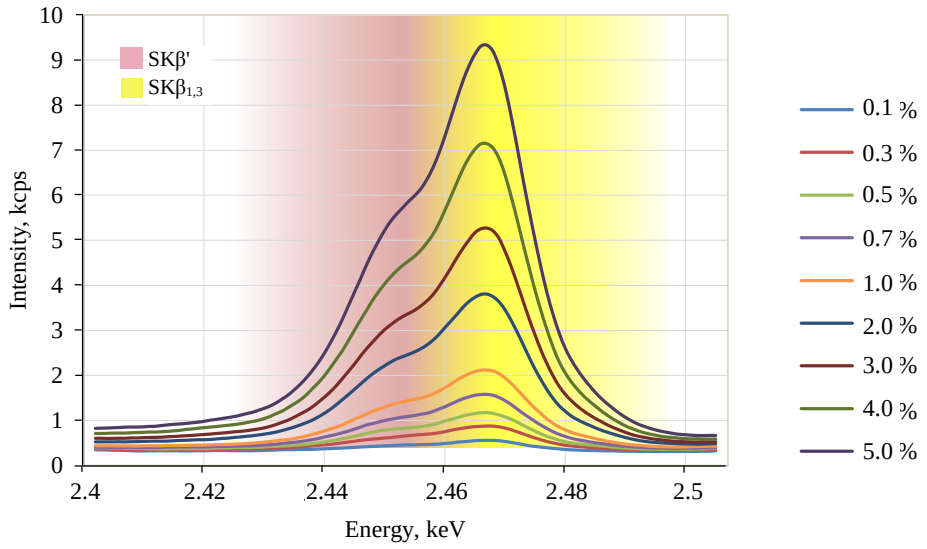

Fig.3. Spectra in the area of the SKβ line

Calibration of the device. To construct the calibration curve, pure anhydrous calcium sulfate was used and mixed with sulfur-free rock dried to an absolutely dry state in the required ratio. A series of samples with different sulfate sulfur content ranging from 0.1 to 5 wt.%, was prepared for calibration. The obtained spectra are shown in Fig.3. For each of the spectra, peaks were selected according to which a calibration curve was built on the intensity of the analytical line and the area under the peak SKβ'. The results of the calibration are shown (Fig.4). As can be seen from the graphs, when calibrating with artificial mixtures, the coefficient of determination is high for both types of calibration: in terms of the intensity of the analytical line and the area under the peak.

Checking the calibration characteristics. To check the calibration characteristics, real objects of various nature: rocks, soils, bottom sediments and mining waste were taken, two of which are standard samples. The content of total sulfur and sulfate sulfur in the selected samples is presented in Table 2. The total sulfur content in the samples varies from 0.10 to 3.44 % and the sulfate content varies from 0.10 to 1.16 % in absolutely dry weight

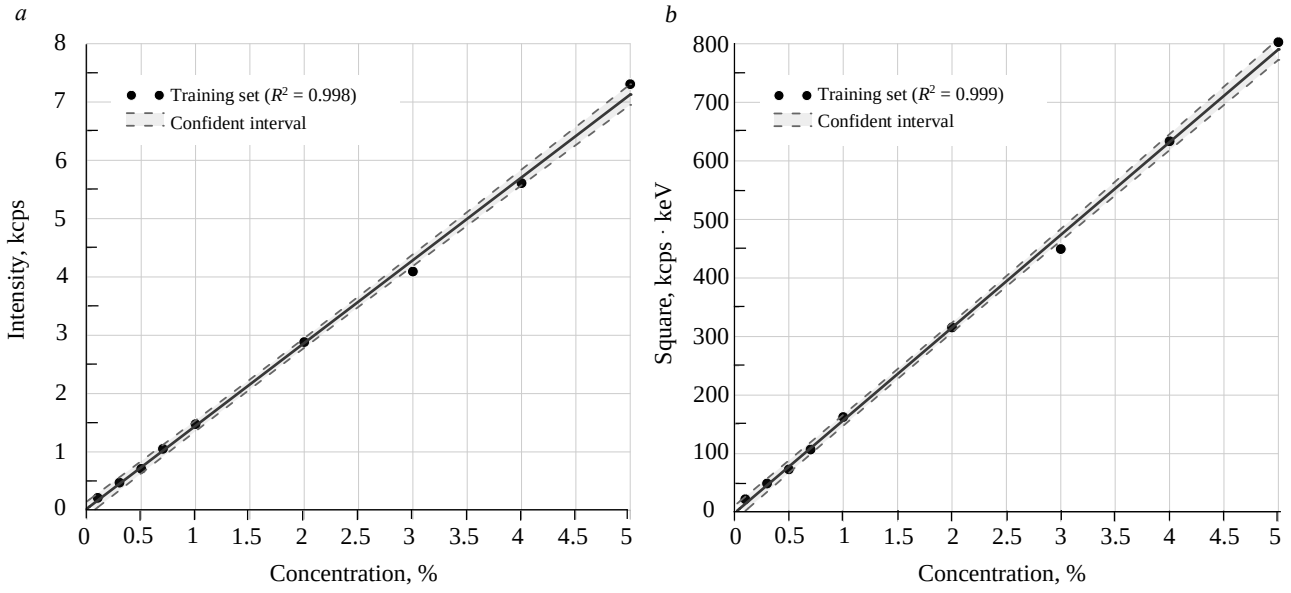

Fig.4. Calibration curves:
a – sulfate sulfur by the intensity of the SKβ′ line; *b* – sulfate sulfur by the area under the SKβ′ peak

Table 2

Samples with known sulfur content, wt.%

Sample	Type	Total sulfur	Sulfate sulfur
SP89	Rock	3.44±0.34	0.18±0.02
SGHM-4	Soil	0.43±0.04	0.23±0.02
1	Mining waste	0.24±0.02	0.23±0.02
2	Mining waste	1.17±0.12	1.16±0.12
3	Bottom sediments	2.14±0.21	0.81±0.08
4	Bottom sediments	0.10±0.01	0.10±0.01
5	Bottom sediments	2.04±0.20	0.73±0.07
6	Bottom sediments	0.61±0.06	0.30±0.03
7	Bottom sediments	0.82±0.08	0.12±0.01
8	Bottom sediments	0.26±0.03	0.24±0.02

The spectra of the SKβ line of rocks, soils, sediments and mining waste after normalization, superimposed on the spectral line of elemental sulfur, are shown in Fig.5. The SKβ' line characteristic of sulfates is observed in each of the samples. For samples 1 and 2, the intensity of the satellite line is the highest, since almost all of the sulfur in these samples is in the form of sulfates. The spectral line of the SP89 sample almost completely coincides with the line of elemental sulfur and only a small part of it in the SKβ' region goes beyond the region of the line of elemental sulfur, since the proportion of sulfate sulfur in this sample is only 5.2 % of the total sulfur. Sample 4 contains the smallest amount of total sulfur, only 0.1 %. For this reason the satellite line is not pronounced in it, despite the fact that all the sulfur in this sample is presented in the form of sulfates.

For all the obtained spectra, the peaks were adjusted (see Fig.2), their maximum intensities and the areas under the peaks were determined, which were later used to determine concentrations by calibration curves (see Fig.4). The results of the analysis are presented in Table 3.

As can be seen from Table 3, the total sulfur content determined by the intensity of the $SK\alpha_{1,2}$ line of sulfate sulfur practically does not differ from the reference values established by the other method. The content of sulfate sulfur determined by the height of the peak and by the area under the peak SKβ' differs significantly for samples with a high content of other forms of sulfur. If the sample contains sulfur only in the form of sulfates, then both methods show themselves to be effective. Calibration by the area under the peak shows better results with samples containing different forms of sulfur, since this method of calibration depends less on the intensity of the main peak $SK\beta_{1,3}$. A similar pattern is observed on the curves of reference concentrations of sulfur from those measured by the X-ray fluorescence method (Fig.6).

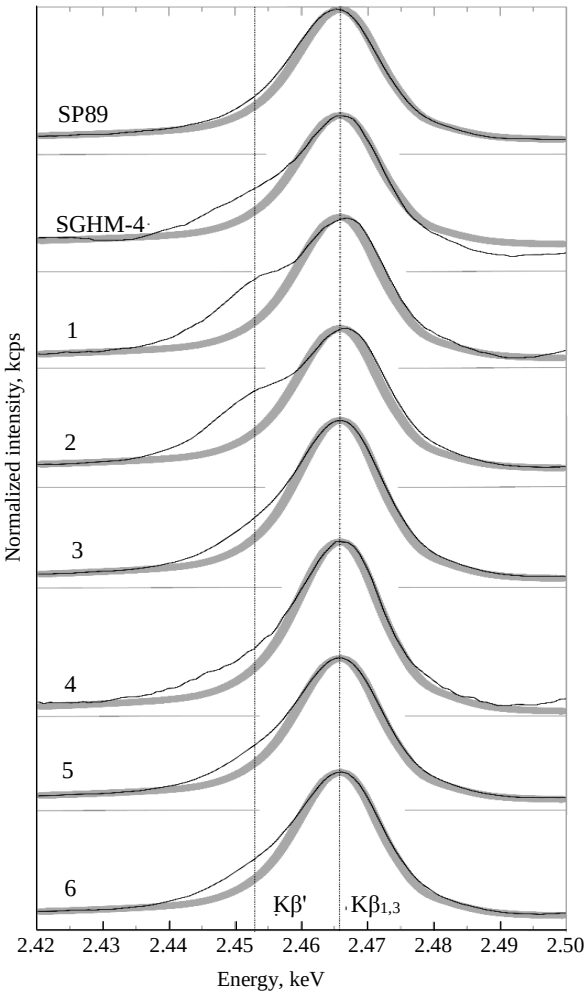

Fig.5. Spectra of various samples superimposed on the SKβ line of elemental sulfur

Journal of Mining Institute. 2024. Vol. 267. P. 372-380

Table 3

The content of total and sulfate sulfur determined by the intensity of the line and the area under the peak, wt.%

Name of the sample	Total sulfur (according to the intensity of the line SK$\alpha_{1,2}$)	Sulfate sulfur (according to the intensity of the SKβ' line)	Sulfate sulfur (by area under the peak SKβ' line)
SP89	3.46	0.58	0.19
SGHM-4	0.42	0.25	0.23
1	0.24	0.27	0.23
2	1.19	1.22	1.19
3	2.14	1.16	1.05
4	0.11	0.11	0.11
5	1.99	1.93	0.82
6	0.64	0.42	0.37
7	0.84	0.22	0.14
8	0.27	0.32	0.28

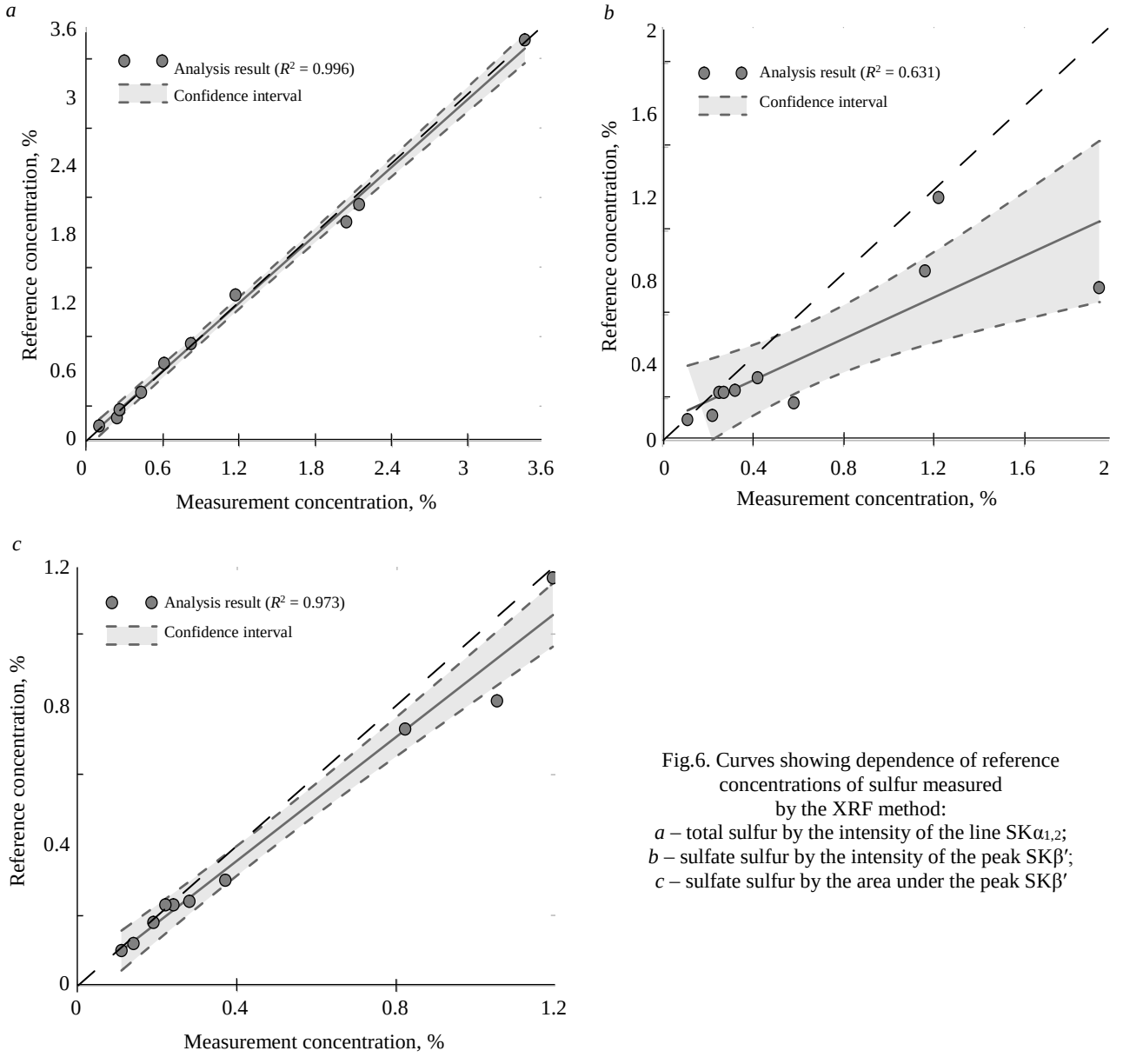

Fig.6. Curves showing dependence of reference concentrations of sulfur measured by the XRF method:
a – total sulfur by the intensity of the line SK$\alpha_{1,2}$;
b – sulfate sulfur by the intensity of the peak SKβ';
c – sulfate sulfur by the area under the peak SKβ'

As can be seen from the graphs of the determination of sulfate sulfur (Fig.6), the theoretical line along which the points of the analysis results must be located goes beyond the confidence interval both when determining by intensity and by area under the peak. Both ranges of confidence intervals go below that theoretical line. This is due to the fact that the separation of SKβ' peaks from $SK\beta_{1,3}$ in case of high non-sulfate sulfur contents is difficult and the measured results exceed the reference values. However. for sulfate sulfur, which was determined by the area under the peak 95 % confidence interval is much smaller, which means that the range of measured values is also smaller [35, 36]. Determination of sulfate sulfur by the area under the peak can be used for rapid assessment of the content of sulfur forms in samples of different nature.

Conclusion. In this study. a new approach to the quantitative assessment of sulfur forms was developed. Calibration curves for the determination of total sulfur were obtained from the intensity of the $SK\alpha_{1.2}$ line, and of sulfates – after processing the $SK\beta_{1,3}$ lines and the SKβ′ satellite line on the X-ray emission spectra after fitting the peaks. With the help of the presented method, it is possible to determine the concentrations of total and sulfate sulfur in ores, mining waste and bottom sediments with a WDXRF spectrometer using calibration curves constructed on the basis of artificial mixtures. The concentrations of sulfate sulfur determined by the area under the peak SKβ′ are consistent with the concentrations measured by the classical method. Determination of sulfate sulfur by the area under the peak can be used for rapid assessment of the content of sulfur forms in samples of different nature.

REFERENCES

1. Ivanov A.V., Smirnov Y.D., Lisay V.V., Borowski G. Issues of the Impact of Granulated Sulfur Transportation on the Environmental Components. *Journal of Ecological Engineering*. 2023. Vol. 24. Iss. 6, p. 86-97. DOI: 10.12911/22998993/162558

2. Pashkevich M.A., Duka A.A. Ecological evaluation of top soil polluted with coal dust. *Gornyi zhurnal.* 2023. N 9, p. 68-74 (in Russian). DOI: 10.17580/gzh.2023.09.10

3. Narayan O.P., Kumar P., Yadav B. et al. Sulfur nutrition and its role in plant growth and development. *Plant Signaling & Behavior*. 2023. Vol. 18. Iss. 1. N e2030082. DOI: 10.1080/15592324.2022.2030082

4. Pashkevich M.A., Kulikova Yu.A. Monitoring and assessment of the negative impact of technogenic massives of the mineral and raw complex. *Mining Informational and Analytical Bulletin.* 2023. N 9-1, p. 231-247 (in Russian). DOI: 10.25018/0236_1493_2023_91_0_231

5. Kharko P., Matveeva V. Bottom Sediments in a River under Acid and Alkaline Wastewater Discharge. *Ecological Engineering & Environmental Technology*. 2021. Vol. 22. Iss. 3, p. 35-41. DOI: 10.12912/27197050/134870

6. Galachieva S.V., Makhosheva S.A., Lyutikova L.A., Tlekhugov A.M. A logical approach to building a machine learning model for assessing the sustainable development of mountain areas. *Sustainable Development of Mountain Territories.* 2023. Vol. 15. N 4, p. 921-928 (in Russian). DOI: 10.21177/1998-4502-2023-15-4-921-928

7. Bykova M.V., Alekseenko A.V., Pashkevich M.A., Drebenstedt C. Thermal desorption treatment of petroleum hydrocarbon-contaminated soils of tundra. taiga. and forest steppe landscapes. *Environmental Geochemistry and Health*. 2021. Vol. 43. Iss. 6, p. 2331-2346. DOI: 10.1007/s10653-020-00802-0

8. Chukaeva M.A., Sapelko T.V. Assessment of the ecological state of aquatic ecosystems by studying lake bottom sediments. *Journal of Mining Institute.* 2024, p. 10 (Online first).

9. Legostaeva Ya.B., Gololobova A.G. Bottom Sediments as an Indicator of the Geoecological State of Natural Water Currents. *Ecology and Industry of Russia.* 2022. Vol. 26. N 11, p. 66-71 (in Russian). DOI: 10.18412/1816-0395-2022-11-66-71

10. Maiorov N.F. Sulfur as an indicator for sulfide ores in lithochemical surveying. *Journal of Mining Institute*. 1974. Vol. 64. N 2, p. 83-86.

11. Pharoe B.K., Evdokimov A.N., Gembitskaya I.M., Bushuyev Y.Y. Mineralogy. geochemistry and genesis of the post-Gondwana supergene manganese deposit of the Carletonville-Ventersdorp area. North West Province. South Africa. *Ore Geology Reviews*. 2020. Vol. 120. N 103372. DOI: 10.1016/j.oregeorev.2020.103372

12. Chukaeva M., Petrov D. Assessment and analysis of metal bioaccumulation in freshwater gastropods of urban river habitats. Saint Petersburg (Russia). *Environmental Science and Pollution Research.* 2022. Vol. 30. Iss. 3, p. 7162-7172. DOI: 10.1007/s11356-022-21955-8

13. Vasilenko T., Kirillov A., Islamov A., Doroshkevich A. Study of hierarchical structure of fossil coals by small-angle scattering of thermal neutrons. *Fuel*. 2021. Vol. 292. N 120304. DOI: 10.1016/j.fuel.2021.120304

14. Jinzhan Huang, Zhiqiang Li, Biao Chen et al. Rapid detection of coal ash based on machine learning and X-ray fluorescence. *Journal of Mining Institute.* 2022. Vol. 256, p. 663-676. DOI: 10.31897/PMI.2022.89

15. Popov O., Talovina I., Lieberwirth H., Duriagina A. Quantitative Microstructural Analysis and X-ray Computed Tomography of Ores and Rocks – Comparison of Results. *Minerals*. 2020. Vol. 10. Iss. 2. N 129. DOI: 10.3390/min10020129

16. Streli C., Wobrauschek P., Kregsamer P. X-Ray Fluorescence Spectroscopy. Applications. Encyclopedia of Spectroscopy and Spectrometry. Elsevier, 2017, p. 707-715. DOI: 10.1016/B978-0-12-803224-4.00315-0

17. Uhlig S., Möckel R., Pleßow A. Quantitative analysis of sulphides and sulphates by WD-XRF: Capability and constraints. *X-Ray Spectrometry*. 2016. Vol. 45. Iss. 3, p. 133-137. DOI: 10.1002/xrs.2679

18. Urch D.S. The origin and intensities of low energy satellite lines in X-ray emission spectra: a molecular orbital interpretation. *Journal of Physics C: Solid State Physics*. 1970. Vol. 3. N 6, p. 1275-1291. DOI: 10.1088/0022-3719/3/6/009

19. Pérez P.D., Carreras A.C., Trincavelli J.C. Structure of the sulfur *K* x-ray emission spectrum: influence of the oxidation state. *Journal of Physics B: Atomic. Molecular and Optical Physics*. 2012. Vol. 45. N 2. N 025004. DOI: 10.1088/0953-4075/45/2/025004

20. Deluigi T.M., Riveros J.A. Chemical effects on the satellite lines of sulfur Kβ X-ray emission spectra. *Chemical Physics*. 2006. Vol. 325. Iss. 2-3, p. 472-476. DOI: 10.1016/j.chemphys.2006.01.022

21. 15 – Sulfur. Chemistry of the Elements. Elsevier, 1997, p. 645-746. DOI: 10.1016/b978-0-7506-3365-9.50021-3

22. Loka Bharathi P.A. Sulfur Cycle. Encyclopedia of Ecology. Amsterdam: Elsevier, 2008, p. 3424-3431. DOI: 10.1016/b978-008045405-4.00761-8

23. Deluigi T.M., Perino E., Olsina R., Riveros de la Vega A. Sulfur- and phosphorus-*Kβ* spectra analyses in sulfite. sulfate and phosphate compounds by X-ray fluorescence spectrometry. *Spectrochimica Acta Part B: Atomic Spectroscopy*. 2003. Vol. 58. Iss. 9, p. 1699-1707. DOI: 10.1016/s0584-8547(03)00155-1

24. Tavares T.R., Molin J.P., Alves E.E.N. et al. Towards rapid analysis with XRF sensor for assessing soil fertility attributes: Effects of dwell time reduction. *Soil and Tillage Research*. 2023. Vol. 232. N 105768. DOI: 10.1016/j.still.2023.105768

25. Wen-Zhi Zhao, Bing Lu, Jun-Bo Yu et al. Determination of sulfur in Soils and Stream Sediments by Wavelength Dispersive X-ray Fluorescence Spectrometry. *Microchemical Journal*. 2020. Vol. 156. N 104840. DOI: 10.1016/j.microc.2020.104840

26. Chubarov V., Amosova A., Finkelshtein A. X-ray fluorescence determination of sulfur chemical state in sulfide ores. *X-Ray Spectrometry*. 2016. Vol. 45. Iss. 6, p. 352-356. DOI: 10.1002/xrs.2712

27. Sverchkov I.P., Gembitskaya I.M., Povarov V.G., Chukaeva M.A. Method of reference samples preparation for X-ray fluorescence analysis. *Talanta*. 2022. Vol. 252. N 123820. DOI: 10.1016/j.talanta.2022.123820

28. Kavčič M., Dousse J.-Cl., Szlachetko J., Cao W. Chemical effects in the Kβ X-ray emission spectra of sulfur. *Nuclear Instruments and Methods in Physics Research Section B: Beam Interactions with Materials and Atoms*. 2007. Vol. 260. Iss. 2, p. 642-646. DOI: 10.1016/j.nimb.2007.04.290

29. Karlsson G., Manne R. Molecular Orbital Interpretation of X-Ray Emission Spectra II. Sulfur and chlorine *Kβ* spectra of some inorganic anions. *Physica Scripta*. 1971. Vol. 4. N 3, p. 119-124. DOI: 10.1088/0031-8949/4/3/007

30. Sánchez E., Deluigi M.T., Castellano G. Binding effects in sulfur Kα and Kβ X-ray emission spectra. *Journal of Analytical Atomic Spectrometry*. 2019. Vol. 34. Iss. 2, p. 274-283. DOI: 10.1039/c8ja00345a

31. Pan Liu, Xiaoyan Deng, Xin Tang, Shijian shen. A wavelet-based Gaussian method for energy dispersive X-ray fluorescence spectrum. *Heliyon*. 2017. Vol. 3. Iss. 5. N e00311. DOI: 10.1016/j.heliyon.2017.e00311

32. Hafizh I., Carminati M., Fiorini C. TERA: Throughput-Enhanced Readout ASIC for High-Rate Energy-Dispersive X-Ray Detection. *IEEE Transactions on Nuclear Science*. 2020. Vol. 67. Iss. 7, p. 1746-1759. DOI: 10.1109/TNS.2020.3001459

33. Cruz-Hernandez Y., Chrysochoou M., Wille K. Wavelength dispersive X-ray fluorescence method to estimate the oxidation reaction progress of sulfide minerals in concrete. *Spectrochimica Acta Part B: Atomic Spectroscopy*. 2020. Vol. 172. N 105949. DOI: 10.1016/j.sab.2020.105949

34. Taniguchi K. Chemical-state Analysis by Means of Soft X-Ray Spectroscopy. II. Kβ Spectra for Phosphorus, Sulfur, and Chlorine in Various Compounds. *Bulletin of the Chemical Society of Japan*. 1984. Vol. 57. Iss. 4, p. 915-920. DOI: 10.1246/bcsj.57.915

35. Oldoni H., Tavares T.R., Brasco T.L. et al. Temporal evaluation of soil chemical quality using VNIR and XRF spectroscopies. *Soil and Tillage Research*. 2024. Vol. 240. N 106087. DOI: 10.1016/j.still.2024.106087

36. Adeleke A.K., Montero D.J.P., Olu-lawal K.A., Olajiga O.K. Statistical techniques in precision metrology. applications and best practices. *Engineering Science & Technology Journal*. 2024. Vol. 5. Iss. 3, p. 888-900. DOI: 10.51594/estj.v5i3.944

Authors: **Ivan P. Sverchkov,** *Candidate of Engineering Sciences, Senior Researcher, Sverchkov_IP@pers.spmi.ru, https://orcid.org/0000-0003-4725-0050* (*Empress Catherine II Saint Petersburg Mining University, Saint Petersburg, Russia*), **Vladimir G. Povarov,** *Doctor of Chemical Sciences, Head of Research Project, https://orcid.org/0000-0001-6710-0514* (*Empress Catherine II Saint Petersburg Mining University, Saint Petersburg, Russia*).

The authors declare no conflict of interests.